

CHAPTER IV

RESULTS AND DISCUSSIONS

4.1 Catalyst Characterization

This research studied the biodiesel production in a batch reactor using heterogeneous basic catalyst. In order to investigate the optimum conditions for this reaction, the catalyst preparation were varied with many parameters, such as the amount of K loading and calcination temperature. In addition, the catalysts were characterized by several techniques in order to explain the catalytic activity of the prepared catalyst. For measuring the basic properties of catalyst, the temperature-programmed desorption of CO₂ (CO₂-TPD) was used. XRD analysis was investigated. Moreover, reusability was studied and XRF was used to determine the amount of active species on the prepared and spent catalysts.

4.1.1 X-ray Diffraction (XRD)

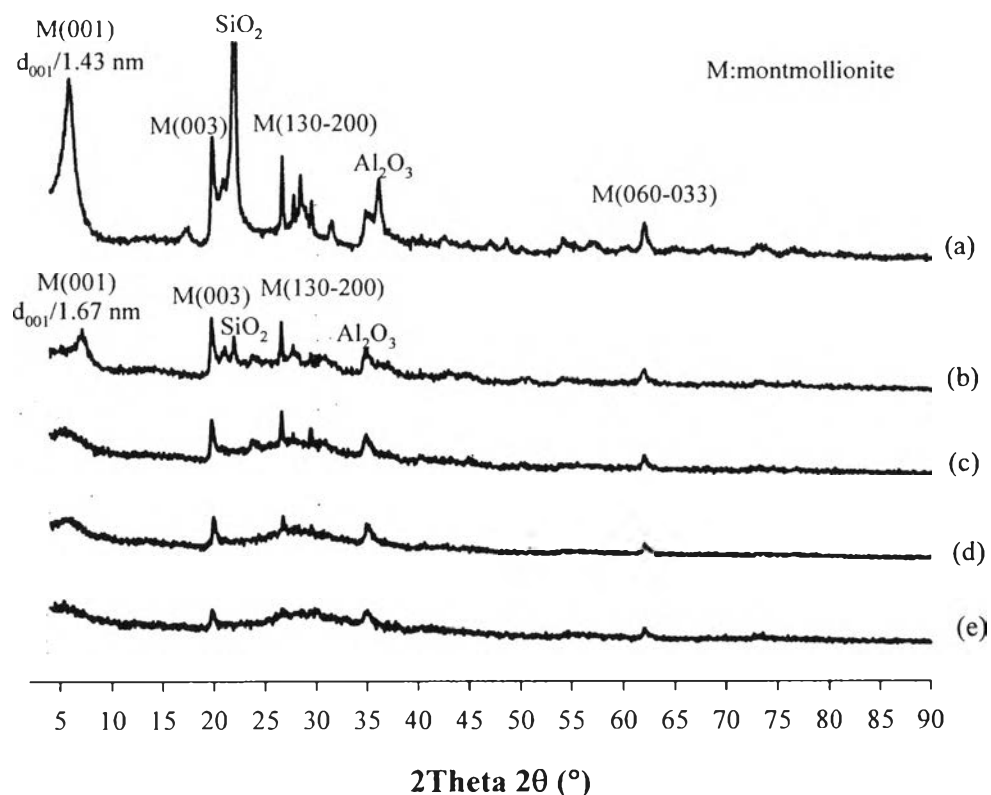


Figure 4.1 XRD patterns of bentonite and K/bentonite catalysts: bentonite (a), 15%K/bentonite (b), 20%K/bentonite (c), 25%K/bentonite (d), 30%K/bentonite (e).

The XRD patterns of fresh bentonite and KOH/bentonite catalysts with different potassium loadings are shown in Figure 4.1. The XRD pattern of bentonite shows diffraction peaks at 5°, 17°, 19°, 21°, 22°, 26°, 28°, 29°, 31°, 34°, 36°, 48°, 54°, and 62°, which contain quartz and bentonite clay. Reflections relative to the planes (001), (003), (130–200), and (060–033) confirmed the presence of montmorillonite in the raw bentonite sample (Soetaredjo *et al.*, 2010). The d_{100} value for raw bentonite was 1.43 nm. As the K loading ratio increased, the crystallinity of the catalyst decreased. When the loading amount of K was increased to 15 wt%, the XRD pattern of the catalyst was still quite similar to that of the raw bentonite sample. The structure of bentonite still could be observed and the d_{100}

value was shifted from 1.43 to 1.67 nm. Reflections at around $2\theta=31^\circ$, 39° , 51° , 55° and 62° attributed to the K_2O phase (Noiroj *et al.*, 2009) are not observed in this work.

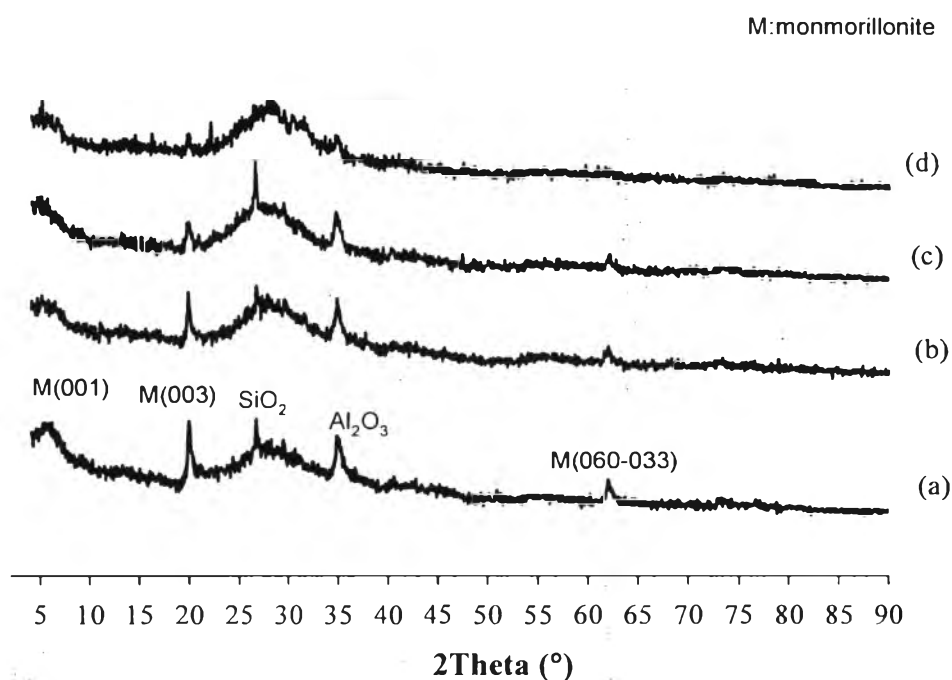


Figure 4.2 XRD patterns of uncalcined 25%K/bentonite catalyst and calcined catalyst at different temperatures: 25%K/bentonite uncalcined (a), 25%K/bentonite calcined at 400°C (b), 25%K/bentonite calcined at 500°C (c), 25%K/bentonite calcined at 600°C (d).

Figure 4.2 illustrates the XRD patterns of 25%K/bentonite at different calcination temperatures (400, 500, and 600 °C). The calcined bentonite is seen to be thermally less stable at temperatures over 400°C. The external components weaken the interaction between the bentonite and thus, thermal instability is induced prior to the complete cleavage of the mesoporous texture (Tabak *et al.*, 2007). When the catalysts were calcined at high temperatures (400 to 600°C), the XRD patterns show the slight reduction of crystallinity due to the collapse of layer.

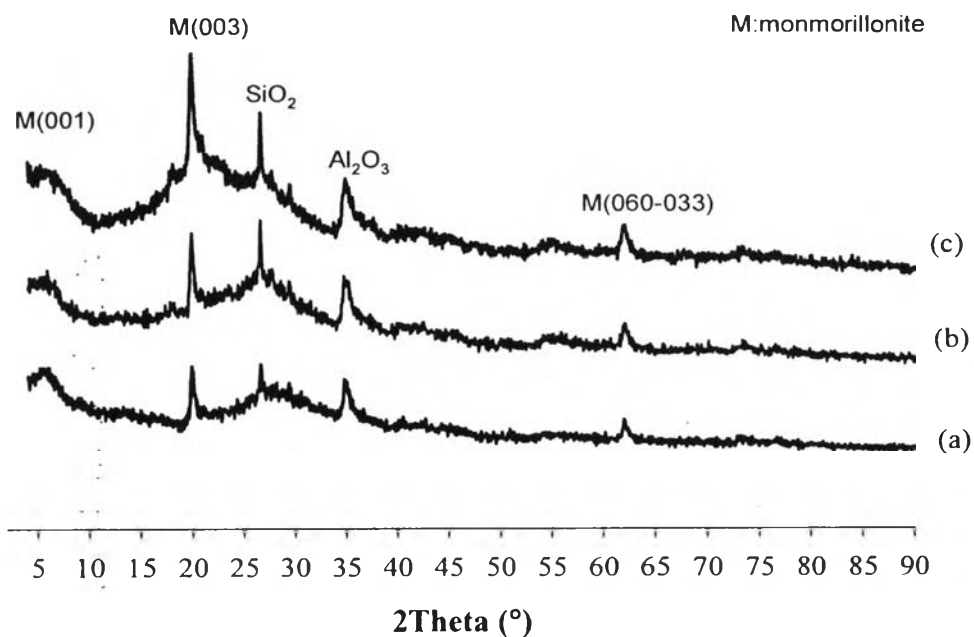


Figure 4.3 XRD patterns of fresh 25%K/bentonite catalyst and spent 25%K/bentonite catalysts: fresh 25%K/bentonite (a), spent^{1st} 25%K/bentonite (b), spent^{2nd} 25%K/bentonite (c).

Figure 4.3 shows the XRD patterns of fresh 25%K/bentonite, spent^{1st} 25%K/bentonite and spent^{2nd} 25%K/bentonite. When the catalysts were tested for 2 cycles: 1st run and 2nd run, the crystallinity of the catalyst slightly increased.

4.1.2 Surface Area Analyzer

Table 4.1 Surface area and pore volume of catalysts

Sample	BET surface area (m ² /g)	Pore Volume (cm ³ /g)
Raw bentonite	48.06	0.111
15%K/bentonite	26.07	0.099
20%K/bentonite	5.86	0.072

The BET surface areas of the catalysts decreased with increasing K loading (Table 4.1). During the impregnation, the KOH molecules filled in the available pores of the bentonite, leading to a decrease of the surface area of the catalyst. By increasing the %wt loading of K, the number of KOH molecules that occupy the available pores in the bentonite also increased, and this phenomenon significantly decreased the BET surface area of the catalyst. Narrowing of the hysteresis curve of the adsorption isotherm (Figure 4.4) indicated that the change in pore structure of bentonite from a mesoporous material to a nonporous structure after loading with K (Soetaredjo *et al.*, 2010).

The nitrogen sorption isotherms of raw bentonite and its modified form are depicted in Figure 4.4. Raw bentonite, 15%K/bentonite, and 20%K/bentonite possess mesoporous structure as indicated by the presence of hysteresis that lies between adsorption and desorption isotherm curve at relative pressures above 0.5. The raw bentonite and its modified form exhibit type IV isotherms characteristic of mesoporous materials. The hysteresis loop is small and possesses features reminiscent of both the H3 and H1 type. The fact that adsorption appears to be limiting at high P/P₀ suggests that the latter classification is a more valid description. Type H1 hysteresis is usually associated with solids consisting of nearly cylindrical channels or agglomerates or compacts of near uniform spheres (Shumaker *et al.*, 1997). In each case, the hysteresis loop is narrow, with almost

parallel adsorption and desorption branches. This is indicative of pores with regular geometry, while the steep desorption behavior indicates that the dimensions of the pores fall in a narrow range. This is clearly seen in the corresponding pore size distribution which show a very narrow distribution. The BET surface area of raw bentonite, 15%K/bentonite, and 20%K/bentonite are 48.06, 26.07, and 5.86 m²/g, respectively. Total pore volume for raw bentonite is 0.111 cm³/g, while the 15%K/bentonite and 20%K/bentonite have lower pore volume (0.099 and 0.072 cm³/g).

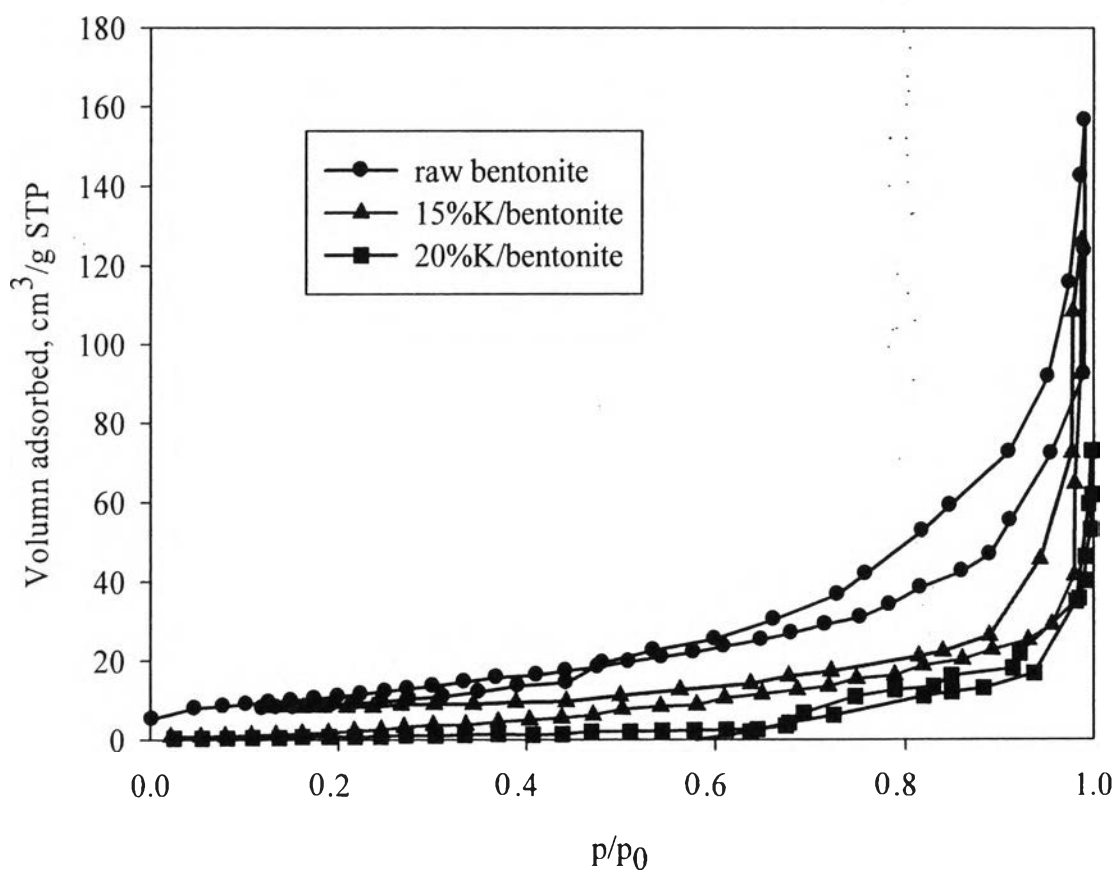
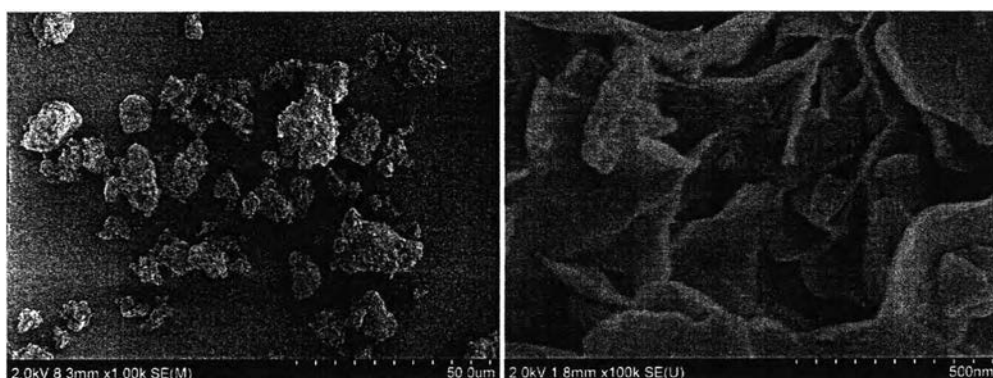


Figure 4.4 Nitrogen sorption isotherms of bentonite and K/bentonite catalysts.

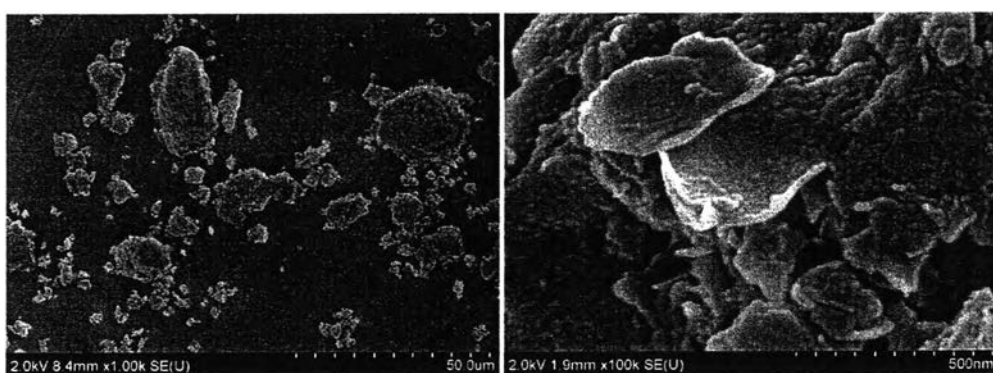
The higher pore volume of raw bentonite compared to 15%K/bentonite and 20%K/bentonite was due to the intercalation of rarasaponin molecules into the structure of bentonite and causing the expansion of interlayer

spacing of bentonite. The pore size distribution of raw bentonite and its modified form was determined by HKP (Horvath Kawazoe Pore sizes) analysis. These catalysts have pore width that distribute mainly from 15 to 80 Å which confirmed the mesoporous nature of adsorbents. This result was in agreement with other previous works (Kurniawan *et al.*, 2010).

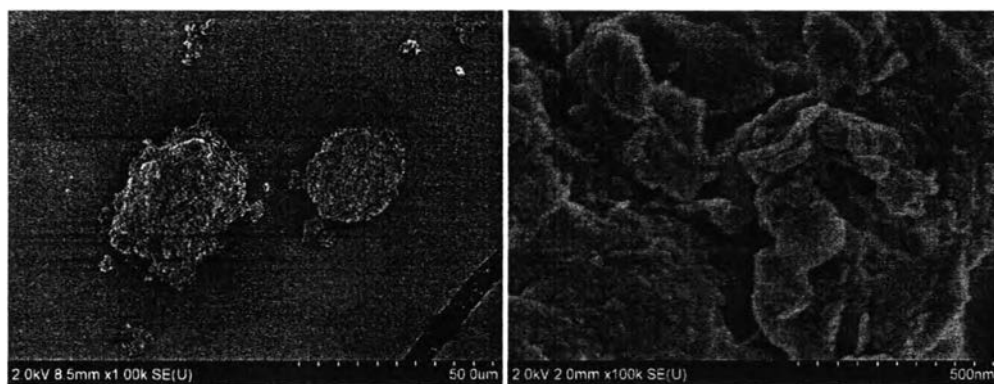
4.1.3 Scanning Electron Microscope (SEM) with Energy Dispersive Spectrometer (EDS)



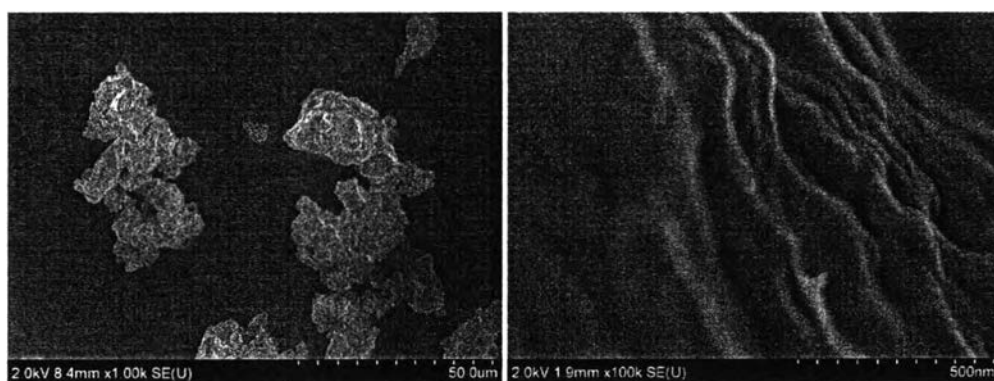
Raw bentonite



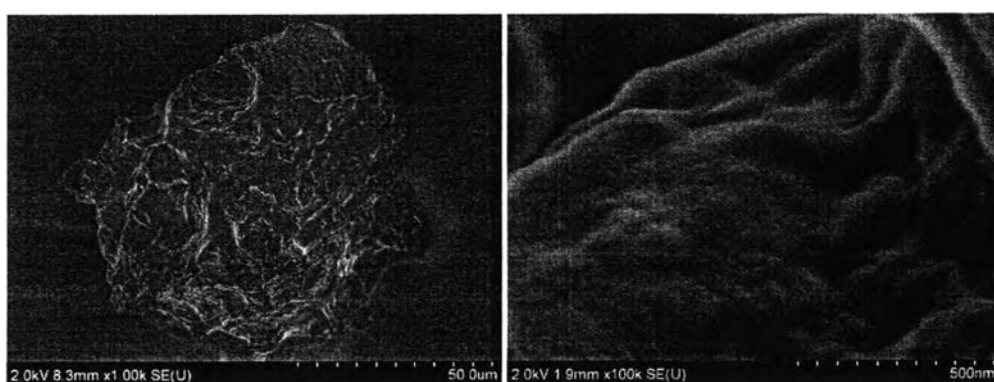
15%K/bentonite



20%K/bentonite

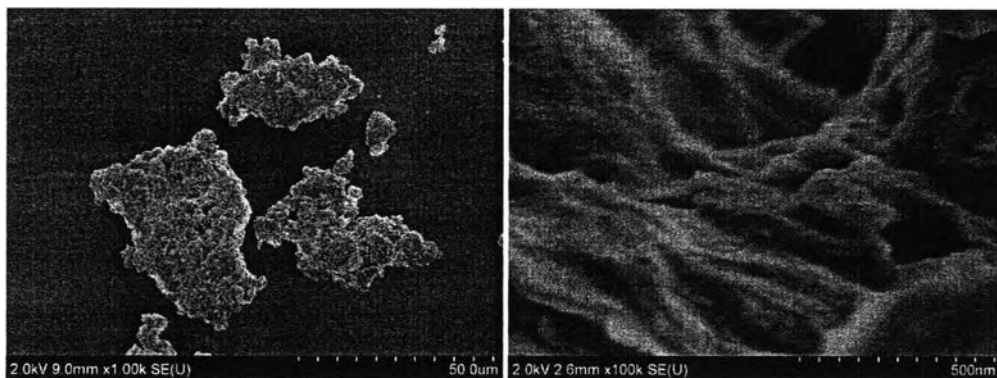


25%K/bentonite

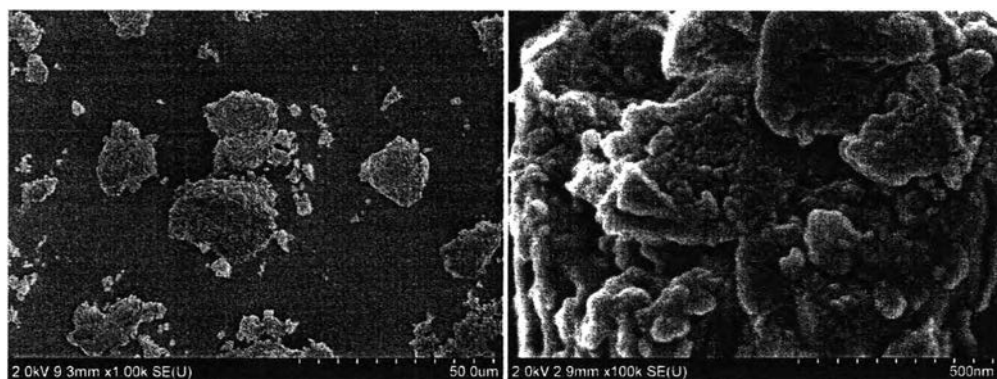


30%K/bentonite

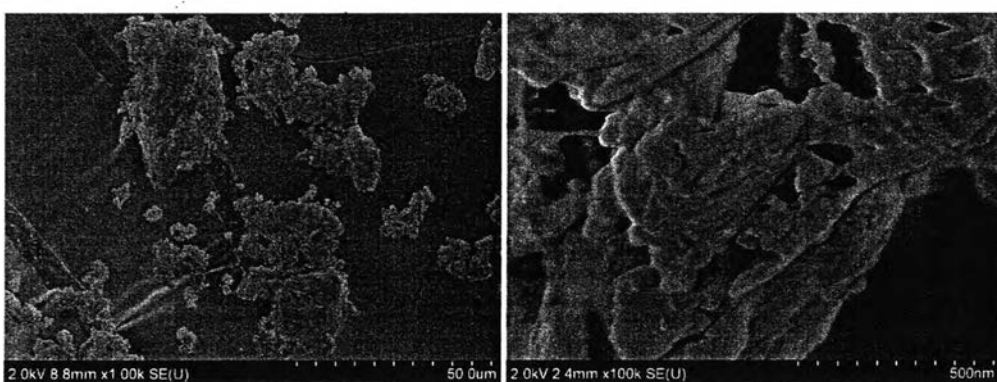




25%K/bentonite Calcined at 400°C



25%K/bentonite Calcined at 500°C



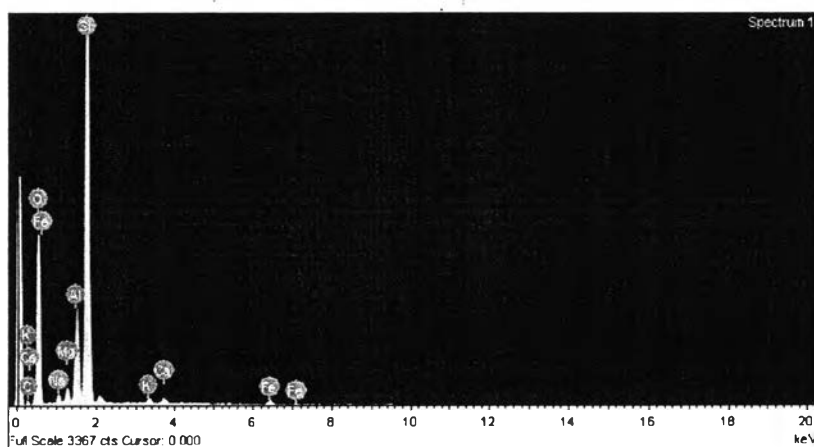
25%K/bentonite Calcined at 600°C



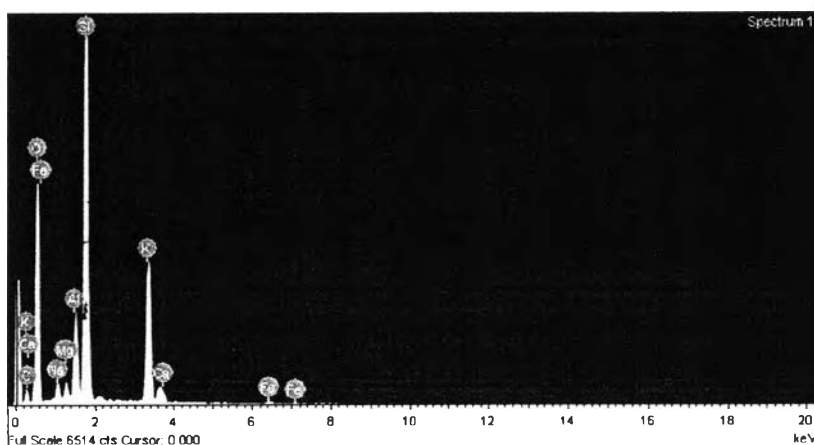
Figure 4.5 SEM micrographs of bentonite and modified bentonite clays.

Scanning electron microscope has extensively been used to examine the morphology and particle size of catalysts. Figure 4.5 shows the SEM micrographs of the pure support and KOH/bentonite catalysts. The particle sizes of raw bentonite, 15%K/bentonite, 20%K/bentonite, 25%K/bentonite, and 30%K/bentonite are 11.71, 19.5, 22.70, 36.25, and 95 μm , respectively. So, the particle size of the catalyst increased when increasing the percent loading of K. This is because the potassium species was highly distributed upon the surface and aggregated to form the higher particle size. This result corresponded to the potassium content measured by EDS.

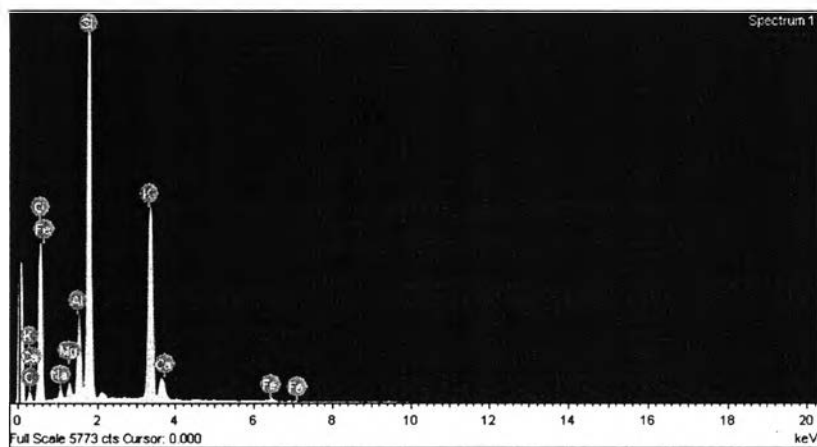
4.1.4 Energy Dispersive Spectrometer (EDS)



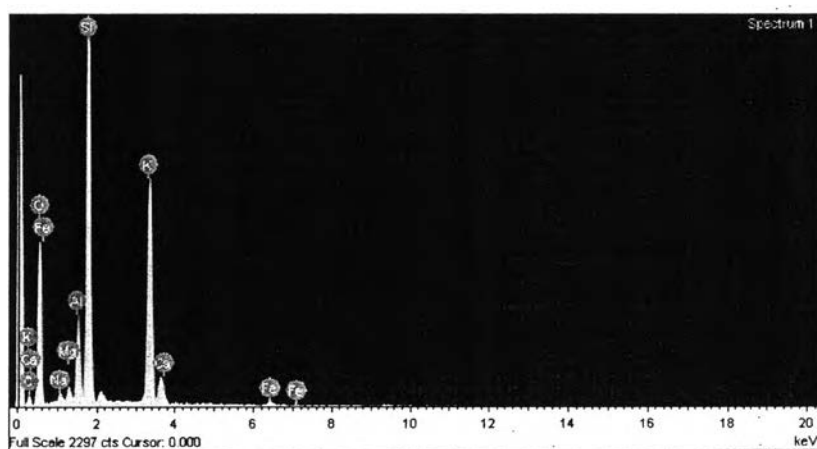
(a) Bentonite



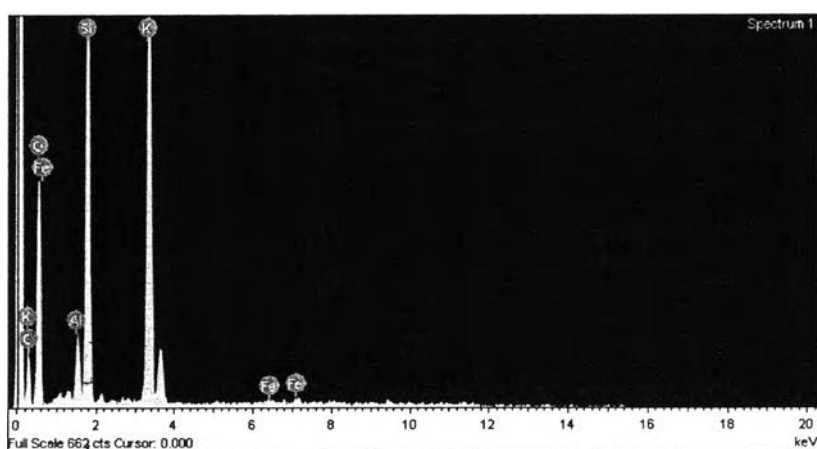
(b) 15%K/bentonite



(c) 20%K/bentonite



(d) 25%K/bentonite



(e) 30%K/bentonite

Figure 4.6 EDS micrographs of pure supports and loading catalysts at 500 \times magnification.

EDS analysis on the composition of bentonite and 15%K/bentonite, 20%K/bentonite, 25%K/bentonite, and 30%K/bentonite is shown in Figure 4.6. Table 4.2 indicates the major composition of bentonite. The potassium content was partially identified by the Energy Dispersive Spectrometer (EDS).

Table 4.2 Composition of bentonite from EDS

Element	Bentonite (%)	15%K/bent (%)	20%K/bent (%)	25%K/bent (%)
C	0.65	0.54	0.40	2.75
O	47.89	51.32	45.27	46.02
Na	0.95	1.19	0.66	0.60
Mg	1.30	0.95	0.85	0.83
Al	7.77	4.66	4.70	4.72
Si	38.09	23.73	24.31	23.45
K	0.95	15.70	22.44	24.83
Ca	0.98	1.03	0.95	0.89
Fe	2.73	0.88	1.22	1.43
Total	100	100	100	100

4.1.5 Hammett Indicator**Table 4.3** Basic strength and basicity of the prepared catalysts

Catalyst	Basic strength (H_+)	Basicity (mmol/g)
Bentonite	$7.2 < H_+ < 9.8$	2.730
15%K/bentonite	$11.0 < H_+ < 15.0$	3.277
20%K/bentonite	$11.0 < H_+ < 15.0$	3.754
25%K/bentonite	$11.0 < H_+ < 15.0$	5.067
30%K/bentonite	$11.0 < H_+ < 15.0$	4.045

Table 4.3 illustrates the basic strength and basicity of the prepared catalysts and as-received bentonite. Basic strength of the catalysts (H_+) was determined by using the following Hammett indicators: bromthymol Blue ($H_+=7.2$), phenolphthalein ($H_+=9.8$), Tropaeolin ($H_+=11$), 2,4-dinitroaniline ($H_+=15$), and 4-nitroaniline ($H_+=18.4$). Bentonite possessed the weak basic strength in a range of ($7.2 < H_+ < 9.8$). After loading potassium from 15 to 30%, the modified catalyst gave a higher basic strength in the range of ($11.0 < H_+ < 15.0$). Nevertheless, it required other titration methods to distinguish the difference of basicity of them. Table 4.3 also shows the basicity from acid titration technique of as-received bentonite and KOH/bentonite catalysts with various potassium loadings. The results revealed that the basicity of prepared catalyst is higher than that of the as-received bentonite clay, and the highest of basicity of catalyst was obtained at 25% potassium. Therefore, it indicated that the basic strength and basicity of the prepared catalyst increased with an increase of potassium loading.

Table 4.4 Activity of fresh and spent catalysts

Sample	Basic strength (H)	Basicity (mmol/g)	Si	Al	Si/Al	K leaching (%)
Fresh 25%K/bentonite	$11.0 < H < 15.0$	5.067	20.735	4.198	4.939	-
Spent ^{1st} 25%K/bentonite	$11.0 < H < 15.0$	5.004	24.446	4.825	5.066	23.848
Spent ^{2nd} 25%K/bentonite	$11.0 < H < 15.0$	4.077	26.004	4.784	5.436	62.744
Spent ^{3rd} 25%K/bentonite	$11.0 < H < 15.0$	5.064	20.256	4.131	4.903	17.892

Table 4.4 shows the basic strength and basicity of the fresh 25%K/bentonite and 25%K/bentonite catalysts tested by repeat the reaction 2 times: 1strun, 2ndrun. After the reusability was tested by repeat the reaction 2 times, the catalyst 1strun and 2ndrun gave a higher basic strength in the range of ($11.0 < H < 15.0$) compared to the basicity from acid titration technique of fresh 25%K/bentonite, spent^{1st} 25%K/bentonite and spent^{2nd} 25%K/bentonite catalysts with various run time of reaction are measured. The results revealed that the basicity of fresh 25%K/bentonite catalyst is higher than those of the spent^{1st} 25%K/bentonite and spent^{2nd} 25%K/bentonite catalysts. Therefore, it indicated that the basic strength and basicity of the spent catalyst decreased with an increase of run time of reaction.

The different Si/Al ratios indicated that the structure of catalyst was changed. The leaching of potassium was investigated by XRF. The optimum conditions for 25%K/bentonite were 3 h reaction time, 15:1 methanol to oil molar ratio, 3 g of catalyst, 300 rpm stirrer speed, and 60°C. At the optimum conditions, a biodiesel yield of 94.13% was obtained. By using the optimum conditions, about 23.85 and 62.74% of the K was leached from spent^{1st} 25%K/bentonite and spent^{2nd} 25%K/bentonite, respectively. Potassium leaching was loss when the spent catalyst was retested and it was found that biodiesel yield was decreased. It could be suggested that potassium was dissolved in reaction mixture and leached out.

4.1.6 Fourier Transform Infrared Spectrophotometer (FT-IR)

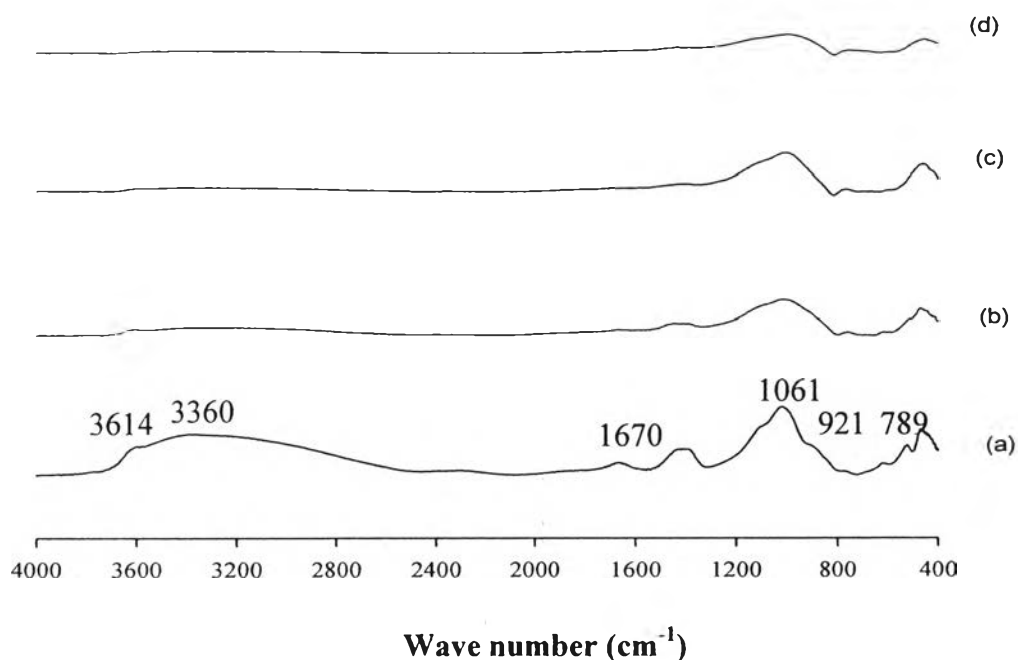


Figure 4.7 FTIR spectra of 25%K/bentonite (a), 25%K/bentonite calcined at 400°C (b), 25%K/bentonite calcined at 500°C (c), and 25%K/bentonite calcined at 600°C (d).

The potassium loaded on bentonite and potassium loaded on bentonite calcined at different temperatures were compressed into a disc using KBr and scanned through infrared spectrometer from 4000 cm^{-1} to 400 cm^{-1} to obtain infrared absorption spectra, as shown in Figure 4.7. It reveals the presence of functional groups such as Al(Mg)–O–H stretching (3614 cm^{-1}), H–O–H stretching (3360 cm^{-1}), H–O–H bending (1670 cm^{-1}), Si–O–Si stretching (1061 cm^{-1}), OH bending bounded Fe^{3+} and Al^{3+} (921 cm^{-1}), and Si–O stretching (789 cm^{-1}). FTIR analysis showed that the addition of KOH affected the structure of the bentonite network. A band at about 3430 cm^{-1} indicates the presence of the stretching vibration of the Al–O–K group (Xie and Lie, 2006).

The peak at 1061 cm^{-1} can be Si-O-Si stretching and peak at 3360 cm^{-1} can be H-O-H stretching group due to potassium hydroxide loaded on bentonite. This Figure represented that the peak of H-O-H stretching group, which obtained from calcined catalysts, is removed due to the adsorbed water molecule in the catalysts would be evaporated when perform the calcination. Whereas the peak of Si-O-Si stretching tend decreased as a calcined temperature increased. This phenomena implied that the Si-O-Si stretching bond can be destroyed by calcination temperature.

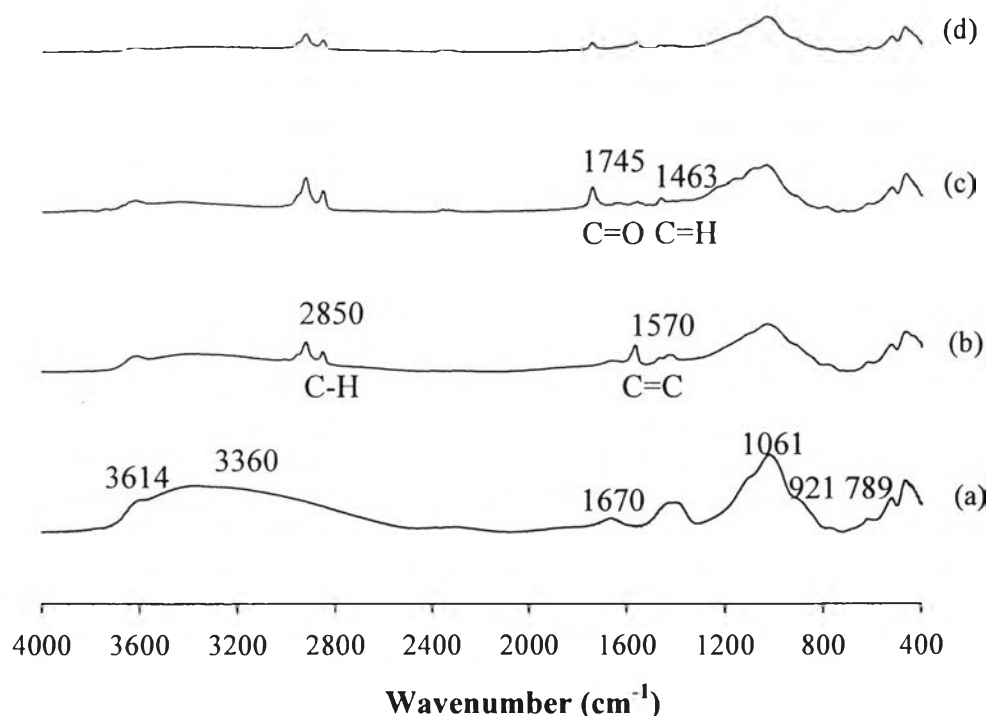


Figure 4.8 FTIR spectra of fresh 25%K/bentonite (a), spent^{1st} 25%K/bentonite (b), spent^{2nd} 25%K/bentonite (c), spent^{3rd} 25%K/bentonite (d).

When the 25%K/bentonite catalyst tested for 2 cycles was tested by FTIR, it was found that the new peak at 2850 cm^{-1} can be C-H stretching, peak 1745 cm^{-1} can be C=O stretching, 1570 cm^{-1} can be C=C stretching, and peak at 1463 cm^{-1} can be C-H stretching which obtained methyl ester, deacylated carbonyl group, aromatic compound, and alkyl group, respectively. Whereas the peak of C-H

stretching, C=O stretching, C=C stretching, and C-H stretching tend to increase as the times of run increased. The phenomena implied that the amount of C-H, C=O, C=C, and C-H stretching increased when the catalyst was tested for 2 times.

4.1.7 Temperature-Programmed Desorption of CO₂ (CO₂-TPD)

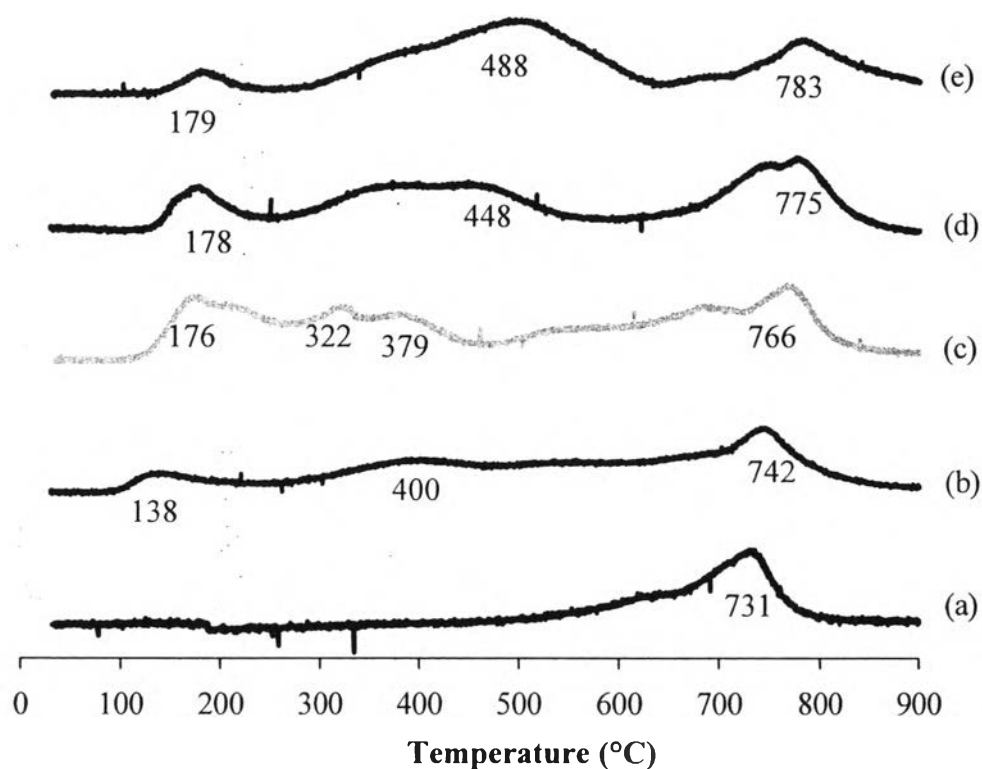


Figure 4.9 TPD profiles of CO₂ on bentonite (a), 15%K/bentonite (b), 20%K/bentonite (c), 25%K/bentonite (d), and 30%K/bentonite (e).

The basic sites for KOH/bentonite is evident from the presence of three TPD signals with T max at 178, 448, and 775°C. The amount of evolved CO₂ corresponding to each band was obtained by integration. Increased K loading are known to possess basic sites of weak, medium and high strength, corresponding to the amount of CO₂ adsorption (Shumaker *et al.*, 2008). T max at 178, 448, and 775°C possessed basic sites of weak, medium and high strength, respectively. The

25%K/bentonite possessed is the highest concentration of strong basic sites at 775°C. The high basicity of 25%K/bentonite at 775°C explains the highest activity for transesterification. It can be concluded that potassium hydroxide can increase both basic strength and basicity of the catalysts. Moreover, basic strength has the same trend compared to Hammett indicator results.

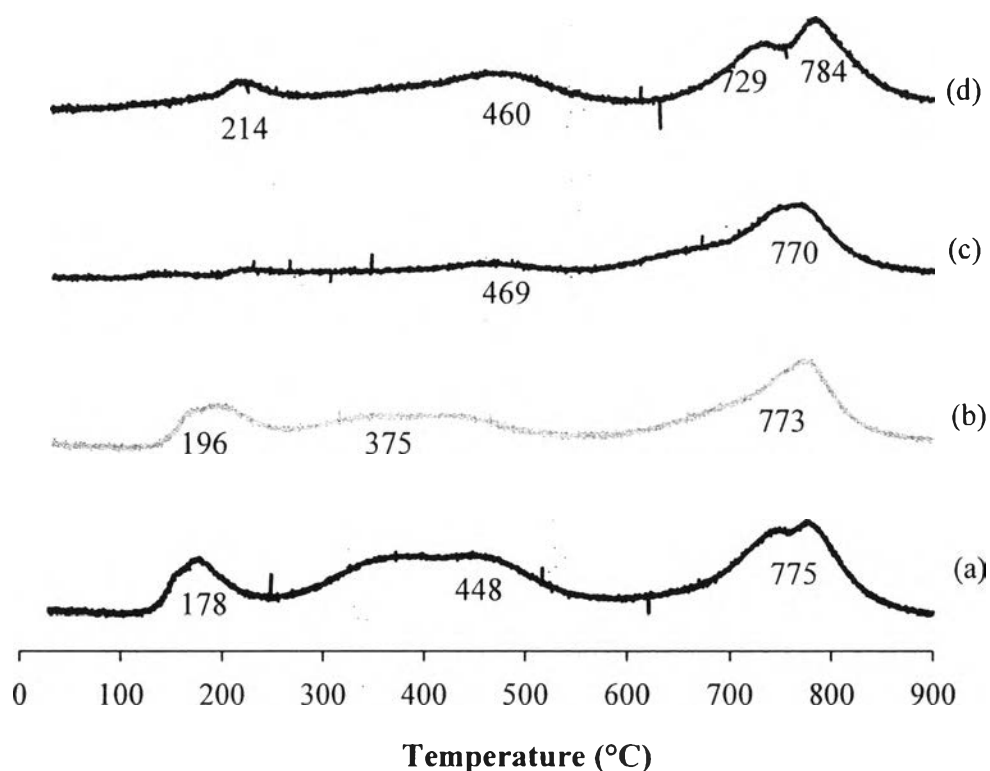


Figure 4.10 CO₂-TPD spectra of calcined catalyst and uncalcined catalyst: 25%K/bentonite uncalcined (a), 25%K/bentonite calcined at 400°C (b), 25%K/bentonite calcined 500°C (c), 25%K/bentonite calcined 600°C (d).

This figure shows basic strength and basic strength of calcined and uncalcined catalysts. It is clearly seen that when the calcination temperature was increased, the basic strength decreased. It could be suggested that calcination process reduce the basic strength of catalyst. However, calcination increase basicity of weak basic strength.

4.2 Transesterification Reaction

KOH/bentonite was used as heterogeneous catalyst in transesterification reaction. To study the optimum condition of these catalysts in transesterification of palm oil. The starting condition of transesterification reaction in KOH/bentonite catalyst was 60°C of the reaction temperature at 300 rpm of stirrer speed, 25 wt% K/bentonite, 15:1 molar ratio of methanol to oil, amount of catalyst 3 wt% (based on weight of vegetable oil).

4.2.1 Effect of wt% Loading of K on Bentonite Support on Biodiesel Yield

To investigate the effect of KOH loading on biodiesel yield, the catalysts were prepared with different potassium loadings in the range of 15–30 wt% of K on bentonite support. At temperature of 60°C, the reaction time was 3 h, 15:1 of molar ratio of methanol to oil, amount of catalyst 3 wt%, and 300 rpm of stirrer speed. The results are presented in Figure 4.11, the biodiesel yield increased with an increase of K loading. The maximum of biodiesel yield of 94.13% was obtained from 25 wt% loading of K on bentonite. However, when the amount of potassium was over 25 wt%, the biodiesel yield decreased. It is believed that the agglomeration of the active KOH phase or the covering of the basic sites by the excess KOH resulted in a lower surface area of the catalyst which could explain their lower activity.

In addition, the product distribution in the esteric phase for the run performed at 60°C in the presence of KOH/bentonite was determined by GC analysis. When the methyl ester increased, the mono-, di-, and tri-glycerides were decreased because these three types of glyceride are converted to methyl ester (Noiroj *et al.*, 2009).

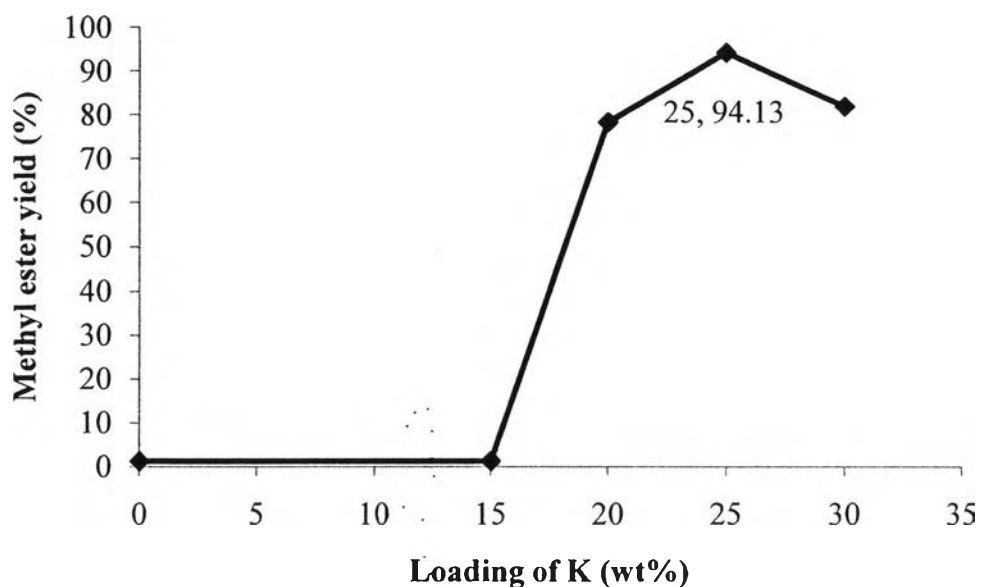


Figure 4.11 Effect of wt% loading of K on bentonite support on biodiesel yield. Reaction conditions: 60°C of reaction temperature, 3 h of reaction time, 15:1 of molar ratio of methanol to oil, amount of catalyst 3 wt%, and 300 rpm of stirrer speed.

4.2.2 Effect of Calcination Temperature on Biodiesel Yield

To investigate the effect of calcination temperature on their catalytic activity, the reaction was fixed at the reaction temperature of 60°C, 300 rpm of stirrer speed. The reaction time was 3 h, and wt% loading of K was obtained from 4.1.1. The calcination temperature of KOH/bentonite was varied from 400 to 600°C. The results are presented in Figure 4.12. It was found that the biodiesel yield decreased when the calcination temperature was increased.

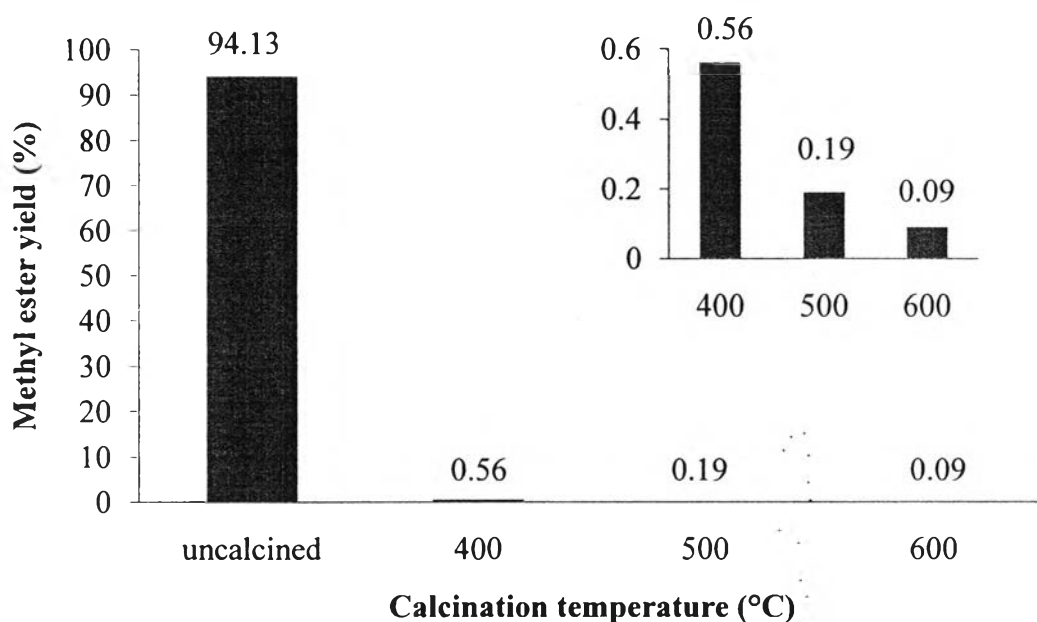


Figure 4.12 Effect of calcination temperature on biodiesel yield.

Reaction conditions: 25%K/bentonite, 60°C of reaction temperature, 3 h of reaction time, 15:1 of molar ratio of methanol to oil, amount of catalyst 3 wt% and 300 rpm of stirrer speed.

4.2.3 Reusability of Catalyst

To find an effective of catalyst, the catalyst was kept to run reaction again. reusability are very important criteria for industrial application of KOH/bentonite as a heterogeneous catalyst for biodiesel production (Soetaredjo et al., 2010). The fresh catalyst or the first cycles run tranesterification reaction. The spent^{1st} catalyst was obtained from the first cycles without pretreatment. The spent^{2nd} catalyst was obtained from the second cycles without pretreatment. And the reimpregnated catalyst was obtained from the spent^{2nd} catalyst reimpregnation or the three cycles. In this study the reusability of KOH/bentonite catalyst was examined by carrying out three reaction cycles. For fresh catalyst (25%K/bentonite) the maximum conversion was 87.77%. After separation from the liquid mixture (biodiesel, glycerin, methanol, and water), the catalyst was tested by repeat the four reaction cycles. A subsequent cycle was started with fresh reactants. For the second, the third cycles, and the fourth cycles, the maximum yield of biodiesel was less than 87.77 (Figure 4.13). It implies that deactivation of basic sites occurred or some of the

possible basic sites were poisoned during the transesterification reaction. These results are similar to those obtained by Soetaredjo *et al.*, 2010.

The fresh catalyst or the first cycles gave biodiesel yield of 87.77%. However, it was found that for the second cycles and the third cycles the biodiesel yield was decreased from the first cycles and gave biodiesel yield of 35.4% and 0.83%, respectively. But, the fourth cycles, the catalyst was reimpregnated, was tested, biodiesel yield increased from the second cycles and the third cycles, and gave the biodiesel yield of 59.31%. The results are shown in Figure 4.13.

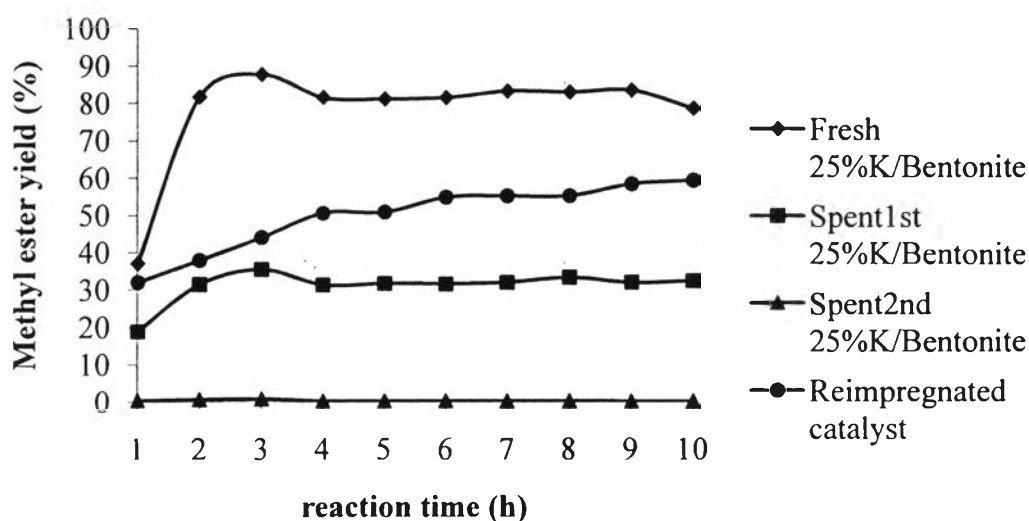


Figure 4.13 Multiple cycle test of catalyst deactivation. Reaction conditions: 25%K/bentonite, 60°C of reaction temperature, 3 h of reaction time, 15:1 of molar ratio of methanol to oil, amount of catalyst 3 wt% and 300 rpm of stirrer speed.

It could be suggested that the active component dissolve in the liquid phase during the reaction so that in the next run the catalyst has less active component to catalyze the reaction.

The methyl ester yield of fresh 25%K/bentonite reaction was analyzed by GC. The methyl ester yield of biodiesel as a function of time is shown in Figure 4.13. The methyl ester was increased when the reaction time was increased and the methyl ester is then constant. The highest methyl ester yield of 87.77 wt% was obtained.

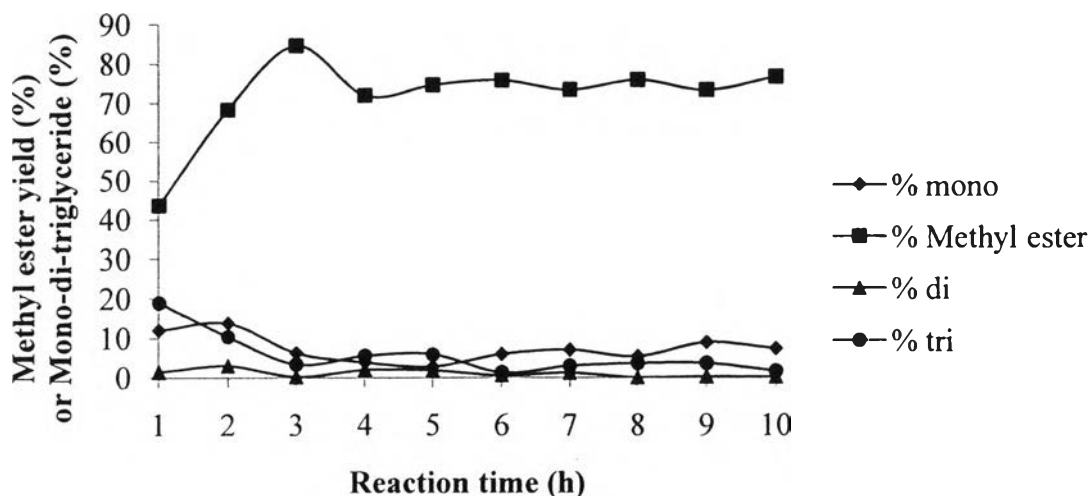


Figure 4.14 Methyl ester yield, mono-, di-, and tri-glycerides of biodiesel as a function of reaction time. Reaction conditions: 25%K/bentonite, 60°C of reaction temperature, 3 h of reaction time, 15:1 of molar ratio of methanol to oil, amount of catalyst 3 wt% and 300 rpm of stirrer speed.

In the same way, the product distribution in the esteric phase over of fresh 25%K/bentonite was determined by HPLC analysis. The methyl ester yield, mono-, di-, and tri-glycerides of biodiesel as function of time is shown in Figure 4.14. It was found that methyl ester increased when the reaction time was increased and the highest methyl ester yield of 84.63% was obtained. But mono-, di- and tri-glycerides content decreased when increasing the reaction time since transesterification consists of a sequence of three consecutive and reversible reactions. In the first step, tri-glyceride is converted to diglyceride. In the second, diglyceride is converted to monoglyceride, and then monoglyceride is converted to glycerol. For each step, one molecule of methyl ester is liberated, so when the methyl ester increased, the mono-, di- and tri-glycerides were decreased because these three types of glyceride are converted to methyl ester.